Dental Materials 40 (2024) 1296–1304

Contents lists available at ScienceDirect

Dental Materials

journal homepage: www.elsevier.com/locate/dental

NP-12 peptide functionalized nanoparticles counteract the effect of bacterial lipopolysaccharide on cultured osteoblasts

Manuel Toledano-Osorio [a], Elvira de Luna-Bertos [b,c], Manuel Toledano [c,d], Francisco Javier Manzano-Moreno [c,d,e,*], Concepción Ruiz [b,c,f], Mariano Sanz [g], Raquel Osorio [c,d]

[a] Postgraduate Program of Specialization in Periodontology, Faculty of Dentistry, University Complutense of Madrid, Madrid, Spain
[b] Biomedical Group (BIO277). Department of Nursing, Faculty of Health Sciences, University of Granada, Spain
[c] Instituto Investigación Biosanitaria, ibs. Granada, Granada, Spain
[d] University of Granada, Faculty of Dentistry, Colegio Máximo de Cartuja s/n, Granada 18071, Spain
[e] Biomedical Group (BIO277), Department of Stomatology, Faculty of Dentistry, University of Granada, Spain
[f] Institute of Neuroscience, University of Granada, Centro de Investigación Biomédica (CIBM), Parque de Tecnológico de la Salud (PTS), Granada, Spain
[g] ETEP (Etiology and Therapy of Periodontal and Peri-Implant Diseases) Research Group. University Complutense of Madrid, Madrid, Spain

ARTICLE INFO

Keywords:
Tideglusib
LPS
Osteogenicity
Titanium
Nanopolymers
Osteoblasts

ABSTRACT

Objective: To evaluate whether nanoparticles (NPs) functionalized with Tideglusib (TDg, NP-12), and deposited on titanium surfaces, would counteract the effect of bacterial lipopolysaccharide (LPS) on osteoblasts.
Methods: Experimental groups were: (a) Titanium discs (TiD), (b) TiD covered with undoped NPs (Un-NPs) and (c) TiD covered with TDg-doped NPs (TDg-NPs). Human primary osteoblasts were cultured onto these discs, in the presence or absence of bacterial LPS. Cell proliferation was assessed by MTT-assay and differentiation by measuring the alkaline phosphatase activity. Mineral nodule formation was assessed by the alizarin red test. Real-time quantitative polymerase chain reaction was used to study the expression of Runx-2, OSX, ALP, OSC, OPG, RANKL, Col-I, BMP-2, BMP-7, TGF-β1, VEGF, TGF-βR1, TGF-βR2, and TGF-βR3 genes. Osteoblasts morphology was studied by Scanning Electron Microscopy. One-way ANOVA or Kruskal-Wallis and Bonferroni multiple comparisons tests were carried out ($p < 0.05$).
Results: TDg-NPs enhanced osteoblasts proliferation. Similarly, this group increased ALP production and mineral nodules formation. TDg-NPs on titanium discs resulted in overexpression of the proliferative genes, OSC and OSX, regardless of LPS activity. In the absence of LPS, TDg-NPs up-regulated Runx2, COL-I, ALP, BMP2 and BMP7 genes. OPG/RANKL gene ratios were increased about 2500 and 4,000-fold by TDg-NPs, when LPS was added or not, respectively. In contact with the TDg-NPs osteoblasts demonstrated an elongated spindle-shaped morphology with extracellular matrix production.
Significance: TDg-NPs on titanium discs counteracted the detrimental effect of LPS by preventing the decrease on osteoblasts proliferation and mineralization, and produced an overexpression of proliferative and bone-promoting genes on human primary osteoblasts.

1. Introduction

Dental implants and implant-supported restorations are currently the most employed therapy to replace missing teeth. However, despite their proven long-term survival, this treatment is not free of complications. The incidence of peri-implant diseases (peri-implant mucositis and peri-implantitis (PI)) is frequent after a variable period of function, with reported patient-level prevalence around 20 % [1]. These diseases are chronic inflammatory conditions of the tissues around dental implants in response to pathogenic biofilm accumulation on the implant and prosthetic component surfaces [2].

In peri-implantitis, the bacterial burden, mainly driven by gram-negative bacteria triggers a non-resolved inflammation that leads to progressive destruction of the implant supporting bone [2]. The tissue destruction characterizing peri-implantitis is driven by the host response to bacteria and bacterial products, as the endotoxin lipopolysaccharide

* Correspondence to: Department of Stomatology, Faculty of Dentistry, University of Granada, Colegio Máximo de Cartuja s/n, Granada 18071, Spain.
E-mail addresses: mantoled@ucm.es (M. Toledano-Osorio), elviradlb@ugr.es (E. de Luna-Bertos), toledano@ugr.es (M. Toledano), fjmanza@ugr.es (F.J. Manzano-Moreno), crr@ugr.es (C. Ruiz), marsan@ucm.es (M. Sanz), rosorio@ugr.es (R. Osorio).

https://doi.org/10.1016/j.dental.2024.06.017
Received 7 February 2024; Received in revised form 7 June 2024; Accepted 9 June 2024
Available online 12 June 2024

(LPS) [3]. In fact, LPS not only induces an exacerbated pro-inflammatory response [4], but also reduces osteoblast proliferation [5].

The difficulties in achieving predictive results in the treatment of peri-implantitis and in light of the non-resolving inflammatory nature of these diseases, has prompted the investigation in not only infection control measures, but also the use of immunomodulatory and anti-inflammatory drugs, which could be effectively used as adjuvants to the treatment and prevention of PI.

Tideglusib (TDg) or NP-12 peptide is a glycogen synthase kinase-3β (GSK-3β) inhibitor [6]. GSK-3β is a small protein that: *i*) inactivates Wnt/β-catenin signaling pathway, reducing osteoblast regenerative response [7,8] and *ii*) leads to Toll-like receptor initiated pro-inflammatory cytokines production and activation [9]. Therefore, it is been hypothesized that this Food and Drug Administration (FDA) approved GSK3-β specific inhibitor (NP-12) could be used as a therapeutic agent in inflammatory, bone resorptive disease processes. The main challenge using TDg is how to locally deliver it, since it is a non-hydrophilic and non-stable compound. It has been incorporated into biodegradable collagen sponges, but these results in rapid release of the peptide [10].

Functionalizing the titanium surface of dental implants has been advocated by using chemical techniques to modify implants surfaces, but these techniques involve multiple laboratory steps and high costs [11], what limits their clinical applications. The application of polymeric nanoparticles (NPs) to the titanium implant surface, as an easy in-chair adjuvant to the regular treatment of peri-implantitis is proposed. The use of these non-resorbable NPs has been previosluy proposed as carriers for drug administration because of an increased surface area, excellent loading, and long-term release properties [12,13]. The use of a suspension of polymeric NPs functionalized with TDg (TDg-NPs) onto implant surfaces may facilitate its local sustained delivery, and hence, their potential therapeutic effect [12].

It was, therefore, the objective of this in vitro investigation to evaluate whether TDg doped NPs, applied onto titanium surfaces would counteract the effects of locally applied LPS bacterial endotoxin on the proliferation and differentiation of human primary osteoblasts.

2. Materials and methods

2.1. Specimens' preparation

NPs were produced by the polymerization/precipitation technique using 2-hydroxyethyl methacrylate as backbone monomer, ethylene glycol dimethacrylate as cross-linker and methacrylic acid as functional monomer [14]. For the functionalizing process, 100 mg of NPs, with a diameter of about 220 nm, were immersed in 1 mL of 0.0017 mg/mL TDg (Sigma-Aldrich, Chemie Gmbh, Riedstr, Germany) solution for 2 h at room temperature under constant shaking (12 rpm) (rotator Orbit 300445, JP Selecta, Barcelona, Spain) and left until the solvent was completely evaporated, thus ensuring that all the TDg remains onto the NPs.

Two groups of NPs were prepared for these experiments: (a) Undoped NPs (Un-NPs) and (b) NPs doped with TDg (TDg-NPs). Sterile pure titanium (grade 4 TiD) discs of 6 mm in diameter, with a micro-surface topography comparable to the commercially available OsseoSpeed®, were manufactured and donated by Dentsply Sirona (Mölndal, Sweden). These discs were placed inside the 24-well plate, and covered with 10 μL of the two different nanoparticles suspensions diluted in ethanol (10 mg/mL)[12]. Considering that 200 μL of culture medium is added per well, the final TDg amount per disc was 50 nM [10].

2.2. Cell culture

Bone fragments were collected from young patients during in third molar extraction surgeries. These patients have previously signed an informed consent approved by the Institutional Human Research Ethics Committee (3312/CEIH/2023). These osseous fragments were processed and the obtained primary osteoblasts were maintained in Dulbecco's modified Eagle medium (DMEM; Invitrogen Gibco Cell Culture Products, Carlsbad, CA). After adding 100 IU/mL penicillin (Lab Roger SA, Barcelona, Spain), 2.5 mg/mL amphotericin B (Sigma, St. Louis, MO, USA), 50 mg/mL gentamicin (Braum Medical SA, Jaen, Spain), 1 % glutamine (Sigma), and 2 % HEPES (Sigma) supplemented with 20 % fetal bovine serum (FBS; Gibco, Paisley, UK), cultures were kept in a humidified atmosphere at 37 ∘C with 95 % air and 5 % CO_2. Next, cells were detached from the flask with 0.05 % trypsin (Sigma) and 0.02 % ethylenediaminetetraacetic acid solution (EDTA; Sigma) and then rinsed and re-suspended in culture medium with 10 % FBS (Gibco, Paisley, UK). Previously published methods were used for identifying and characterizing the osteoblasts [15,16].

In these experiments, the three different treated discs (TiD uncovered -control-, TiD covered with Un-NPs or TiD with TDg-NPs) were placed inside the 96-well plates containing the osteoblast cultures. Then cells were incubated in a humid atmosphere 95 % air and 5 % CO_2 at 37 C and after attaining a cell density of 1×10^4 cells mL^{-1} per well, either bacterial lipopolysaccharide endotoxin (LPS) at 1 μg mL^{-1} (Sigma-Aldrich/Merck) or a diluent were added to the cell cultures.

2.3. Cell proliferation assay

After 48 h, cell proliferation was tested using the 3-(4,5-dimethylthiazol-2-yl)− 2,5-diphenyltetrazolium (MTT) assay (Sigma). The media was replaced by phenol red-free DMEM with MTT 0.5 mg/mL and then incubated for 4 h. MTT cellular reduction produced insoluble crystal deposits of formazan, that were dissolved by adding dimethyl sulfoxide (Merck Biosciences, Darmstadt, Germany). Absorbance was then measured with a spectrophotometer (Sunrise, Tecan, Männedorf, Switzerland) at 570 nm [12]. The attained results were expressed as means and standard deviations (SD) of the absorbance values. At least three experiments were performed for each type of nanoparticles.

2.4. Alkaline phosphatase activity measurement

Early osteoblast differentiation was evaluated with the alkaline phosphatase (ALP) activity test using a colorimetric assay that assesses the amount of ALP enzyme present in the culture, by measuring the conversion of the colourless substrate p-nitrophenyl phosphate to the yellow p-nitrophenol (Diagnostic kit 104-LL, Sigma). Various standards of p-nitrophenol (0–250 μM) were prepared and assayed in parallel from dilutions of a 1000 μM stock solution [12]. After 72 h, cell cultures growing on the discs inside the 96-well plates were lysed with 100 μL of triton x-100 and 1 M Tris by ultrasonication for 4 min at pH 8.00. The suspension was then mixed with a 7.6 mM p-nitrophenylphosphate solution, at a proportion of 1:10 and t incubated for 15 min at 37∘C. A substrate solution was prepared by merging an aqueous solution of 4mgmL^{-1} of 4-nitrophenyl phosphate disodium salt (Sigma) with an equal volume of 1.5 M alkaline buffer (Sigma). The reaction was stopped, by adding 1 mL 0.05 N NaOH, and then, the final absorbance was measured with a spectrophotometer at 405-nm (Sunrise, Tecan, Männedorf, Switzerland). The total protein content was estimated by the Bradford method using a protein assay kit from Bio-Rad Laboratories (Bio-Rad Laboratories, Nazareth-Eke, Belgium). Experiments were conducted in triplicate.

2.5. Matrix mineralization evaluation

The deposition of matrix mineralization on the discs was evaluated using the Alizarin Red S method. Primary osteoblast cells were seeded at 5×10^4 cells/mL/well in a 96-well plate, and then cultured in osteogenic medium (DMEM supplemented with 0.05 mM ascorbic acid and 5 mM β-glycerophosphate) on the different experimental conditions (in the presence or absence of LPS) at 37 °C in a humidified atmosphere (95 %

air and 5 % CO_2). After 14d and 21d of culture, the mineral depositions of the cells were evaluated. Ten percent (w/v) cetylpyridinium chloride was used to stop red calcium deposits for 15 min. Their absorbance was measured with a spectrophotometer (BioTek ELx800) at a wavelength of 562 nm [17].

2.6. RNA extraction and real-time polymerase chain reaction (RT-PCR) assessments

After 48 h of culturing, the Qiagen RNeasy extraction kit (Qiagen Inc., Hilden, Germany) was used to extract the mRNA from the osteoblasts. The amount of extracted mRNA was measured by UV spectrophotometry at 260-nm (Eppendorf AG, Hamburg, Germany). Afterwards, 1 μg of mRNA from each group was brought to 40 μL of total volume, reverse-transcribed to cDNA and amplified with iScriptTM cDNA Synthesis Kit (Bio-Rad laboratories, Hercules, CA, USA) by polymerase chain reaction [12].

Once the RNA was reverse transcribed the primers to detect mRNA of: runt-related transcription factor 2 (Runx-2), osterix (OSX), alkaline phosphatase (ALP), osteocalcin (OSC), osteoprotegerin (OPG), ligand for RANK (RANKL), type I collagen (Col-I), bone morphogenetic proteins 2 and 7 (BMP-2 and BMP-7), TGF-β1 and TGF-β receptors (TGF-βR1, TGF-βR2, and TGF-βR3) and vascular endothelial growth factor (VEGF), were selected using the NCBI- nucleotide library and Primer3-design. Results were always normalized using ubiquitin C (UBC), peptidylprolyl isomerase A (PPIA), and ribosomal protein S13 (RPS13) as housekeeping genes [12]. Their sequences are depicted in Table 1.

The RT-qPCR was conducted using the SsoFast™ EvaGreen® Supermix Kit (Bio-Rad laboratories). The obtained cDNA (5 μL per sample) was placed in 96-well microplates and amplified by means of an IQ5-Cycler (Bio-Rad laboratories). The annealing and elongating temperatures were set at 60–65ºC and 72ºC, respectively. Over 40 cycles were performed. The Ct values were plotted against the log cDNa dilution in order to obtain a standard curve for each of the targeted gene. Then, the nonspecific PCR products and primer dimers were ruled out creating a melting profile and carrying out an agarose gel electrophoresis. The results were expressed as the proportion of ng of mRNA per average ng of housekeeping mRNA [12]. The whole process was performed in triplicate.

2.7. Field emission scanning electron microscopy (FESEM)

After 48 h of osteoblasts culturing, two discs of each experimental group were submitted to critical drying point and were covered with carbon. FESEM (GEMINI, Carl Zeiss SMT, Oberkochen, Germany) analysis was performed [12]. Images were taken at 3 kV at a working distance of 4 mm. Low and high magnifications images were taken at 500X or 1000 to 3,000X, respectively.

2.8. Statistical analysis

Data were expressed as means ± standard deviation (SD). Their normality in the distribution was assessed using Kolmogorv–Smirnov tests ($p \geq 0.05$). Mean comparisons were conducted by one-way ANOVA and Bonferroni multiple comparisons for variables fulfilling a normal distribution and by Kruskal-Wallis for non-parametric distributed data. Significance was set at $p \leq 0.05$.

3. Results

3.1. Cell proliferation assay

The results from the MTT assay are presented in Fig. 1, as mean and standard deviations of the osteoblast cells proliferation. TDg-NPs produced a two-fold increase in osteoblasts proliferation, when compared to the control ($p \leq 0.05$). LPS addition half reduced cell proliferation in the controls, but in the presence of TDg-NPs it resulted in a four-fold increase ($p < 0.05$).

3.2. Alkaline phosphatase (ALP) activity

Mean and standard deviations of ALP activity are expressed as international units (IU) of ALP per mg of total proteins and they are shown in Fig. 2. No significant differences were found in ALP production between groups, in the absence of LPS ($p > 0.05$). When LPS was added to cultured cells, ALP production was reduced in half ($p < 0.05$), compared to the control group. When LPS was added in presence of TDg-NPs ALP production was recovered by about 75 %.

3.3. Mineralization assay

The absorbance for the different discs at 14 and 21 d are displayed in Fig. 3. After 14 d of culture, LPS reduced in half osteoblast mineralization ($p < 0.05$), while in the presence of TDg NPs, this effect was reversed ($p > 0.05$). A similar trend occurred after 21d, but in this timing TDg NPs in absence of LPS, resulted in a 30 % increase in mineralization, ($p < 0.05$).

3.4. Real-time quantitative polymerase chain reaction

The Result from the RT-qPCR analysis is displayed in Figs. 4 and 5. In general, LPS addition provoked a down-regulation on the expression of

Table 1
Sequences of Primers for the amplification of osteoblasts' cDNA by real-time polymerase chain reaction.

Gene	Sense Primer (5′–3′)	Antisense Primer
TGFβ1	TGAACCGGCCTTTCCTGCTTCTCATG	GCGGAAGTCAATGTACAGCTGCCGC
TGFβ-R1	ACTGGCAGCTGTCATTGCTGGACCAG	CTGAGCCAGAACCTGACGTTGTCATATCA
TGFβ-R2	GGCTCAACCACCAGGGCATCCAGAT	CTCCCCGAGAGCCTGTCCAGATGCT
TGFβ-R3	ACCGTGATGGGCATTGCGTTTGCA	GTGCTCTGCGTGCTGCCGA TGCTGT
Runx-2	TGGTTAATCTCCGCAGGTCAC	ACTGTGCTGAAGAGGCTGTTTG
VEGF	CCTTGCTGCTCTACCTCCAC	CACACAGGATGGCTTGAAGA
OSX	TGCCTAGAAGCCCTGAGAAA	TTTAACTTGGGGCCTTGAGA
BMP-2	TCGAAATTCCCCGTGACCAG	CCACTTCCACCACGAATCCA
BMP-7	CTGGTCTTTGTCTGCAGTGG	GTACCCCTCAACAAGGCTTC
ALP	CCAACGTGGCTAAGAATGTCATC	TGGGCATTGGTGTTGTACGTC
Col-1	AGAACTGGTACATCAGCAAG	GAGTTTACAGGAAGCAGACA
OSC	CCATGAGAGCCCTCACACTCC	GGTCAGCCAACTCGTCACAGTC
OPG	ATGCAACACAGCACAACATA	GTTGCCGTTTTATCCTCTCT
RANKL	ATACCCTGATGAAAGGAGGA	GGGGCTCAATCTATATCTCG
UBC	TGGGATGCAAATCTTCGTGAAGACCCTGAC	ACCAAGTGCAGAGTGGACTCTTTCTGGATG
PPIA	CCATGGCAAATGCTGGACCCAACACAAATG	TCCTGAGCTACAGAAGGAATGATCTGGTGG
RPS13	GGTGTTGCACAAGTACGTTTTGTGACAGGC	TCATATTTCCAATTGGGAGGGAGGACTCGC

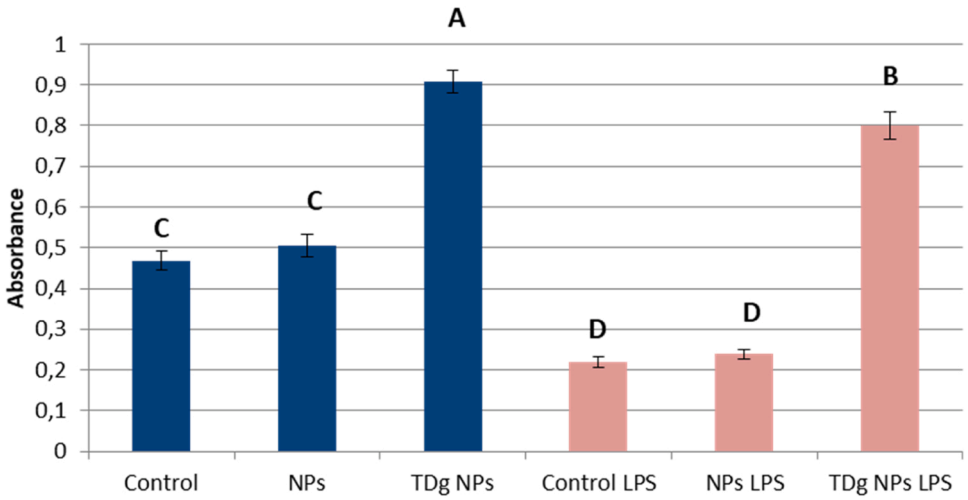

Fig. 1. Mean and standard deviation of absorbance values obtained after the MTT assay for the different experimental groups. Different letters indicate significant differences after ANOVA and post-hoc comparisons ($p \leq 0.05$). Control: titanium discs, NPs: Titanium discs covered with un-doped NPs, TDg NPs: Titanium discs with Tideglusib doped NPs, LPS: 1 μg of bacterial endotoxin was added to cultured cells.

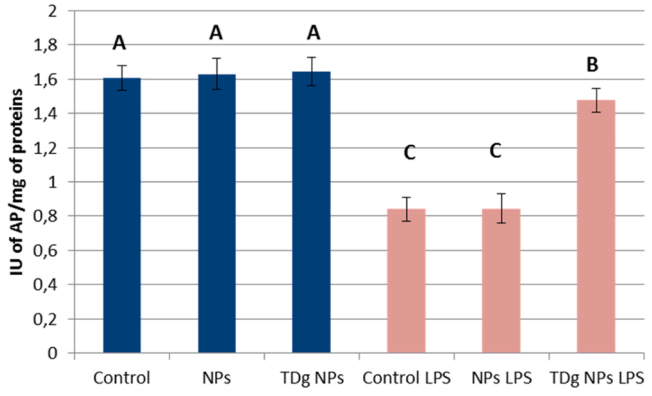

Fig. 2. Mean and standard deviation of international units of ALP per mg of proteins, the values were obtained at the different tested discs. Distinct letter indicates significant differences between groups after ANOVA and post-hoc comparisons ($p \leq 0.05$). Control: titanium discs, NPs: Titanium discs covered with un-doped NPs, TDg NPs: Titanium discs with Tideglusib doped NPs, LPS: 1 μg of bacterial endotoxin was added to cultured cells.

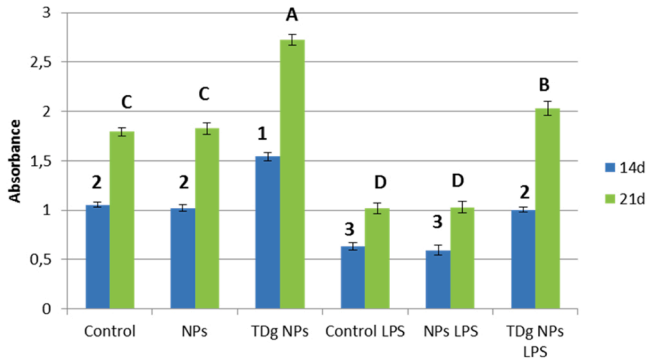

Fig. 3. Mean and standard deviation of absorbance obtained with the different membranes using the Alizarin Red S method. Distinct letter indicates significant differences between groups after ANOVA and post-hoc comparisons ($p \leq 0.05$). Distinct capital letter indicates significant difference between discs in the 14d group and distinct lowercase letter indicates significant difference between discs in the 21d group. Control: titanium discs, NPs: Titanium discs covered with un-doped NPs, TDg NPs: Titanium discs with Tideglusib doped NPs, LPS: 1 μg of bacterial endotoxin was added to cultured cells.

the tested osteogenic and proliferative genes. In contrast, the incorporation of TDg NPs caused an up-regulation of these genes, regardless of LPS presence.

In particular, TDg NPs up-regulated about 3 times the proliferation-related genes TGF-β1, TGF-βR1 and TGF-βR2 if compared to the control titanium discs ($p < 0.05$). After adding LPS these genes drastically decreased ($p < 0.05$), except when TDg NPs was present, which resulted in values similar to the control group ($p > 0.05$). TGF-βR3 was also down-regulated after LPS addition ($p < 0.05$), but in presence of TDg NPs, but, in this case in when added TDg NPs the initial values were only half-recovered ($p < 0.05$).

The osteoblast expression of ALP and Runx-2 was increased in the presence of TDg NPs and in the absence of LPS (about 3-fold increase) compared to the control group; $p < 0.05$). In both cases TDg was not able to rise the gene expression when LPS was present. A similar trend was observed for the gene expression of COL-I, BMP-2 and BMP-7.

When analyzing OSX gene expression, TDg-NPs produced an up-regulation (2-fold increase respect to the control titanium discs). In LPS-treated osteoblasts OSC and OSX expression were reduced and TDg could counteract the effect in both cases.

TDg NPs groups attained a marked up-regulation of the expression of OPG that was six and three-fold in the absence and presence of LPS, respectively. In the control groups, OPG gene expression was not affected by LPS ($p > 0.05$). RANKL expression was decreased about 20 times when TDg or LPS were present ($p < 0.05$). The OPG/RANKL ratio was significantly higher when TDg NPs were present, regardless of the action of LPS. VEGF gene expression was decreased when LPS was in the media and TDg-NPs were not able to reverse this effect.

3.5. *Scanning electron microscopy*

Selected images from the SEM analysis of the six groups are displayed in Figs. 6 and 7, using different magnifications. When osteoblasts were grown on titanium discs, the complete surface was covered by flat and polygonal cells, also depicting their inter-cellular connections (Figs. 6A and 7A). Osteoblasts grown on Ti discs with NPs were like the control group, although with slightly elongated shapes and depicting for more cells surface deposits (Figs. 6B and 7B). Similarly, when TDg NPs were present, osteoblasts were elongated in shape showing mineral deposits on their surface (Figs. 6C and 7C). After LPS addition, cells membranes were disrupted (Figs. 6D and 7D). In presence of LPS without TDg NPs the number of cells diminished cells (Figs. 6D to E and 7D to E). In presence of TDg NPs and LPS, the disk titanium surface is

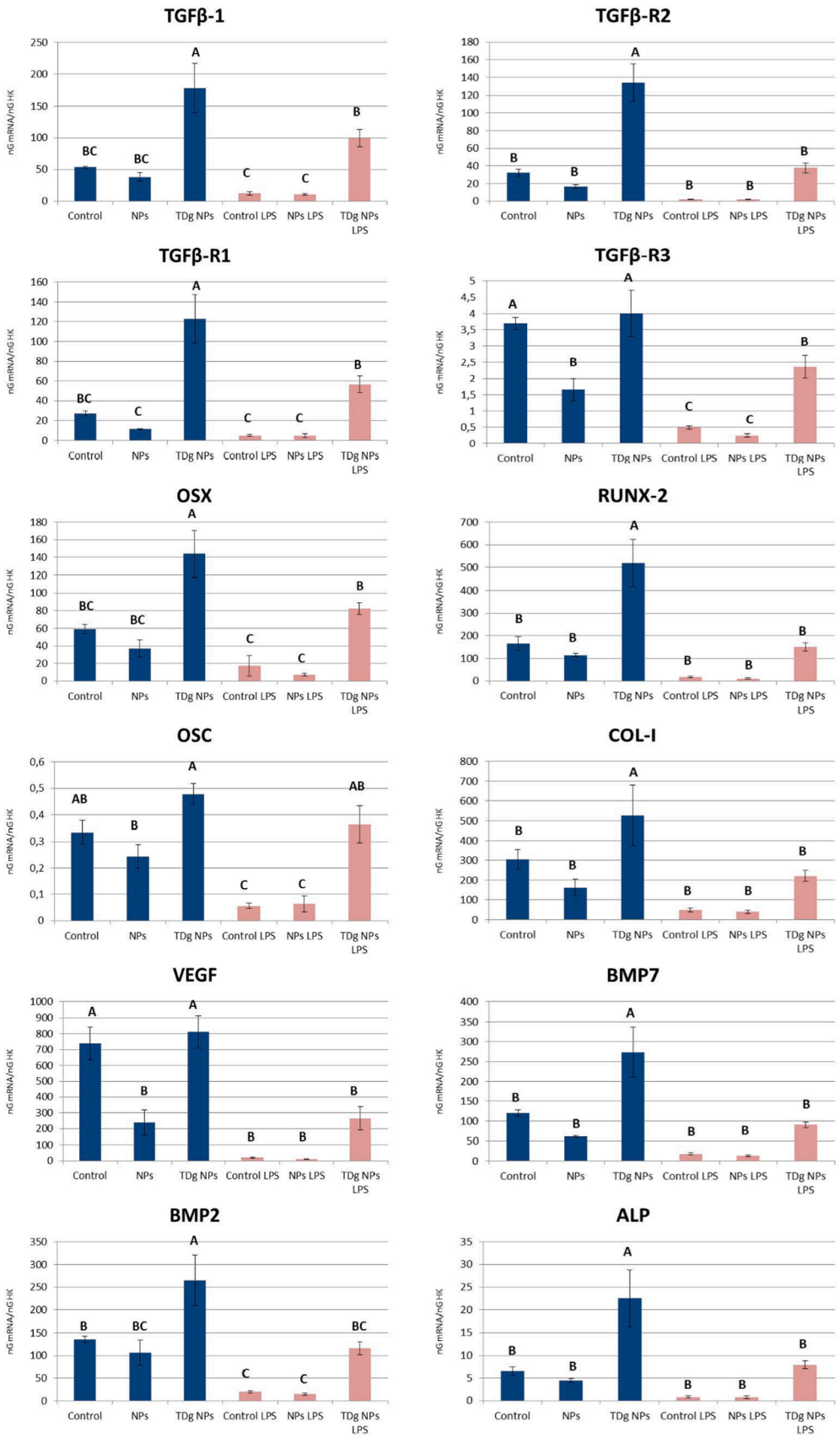

(caption on next page)

Fig. 4. Quantitative real-time PCR gene expression analysis of TGFβ-1, TGFβ-R1, TGFβ-R2, TGFβ-R3, VEGF, OSC, OSX, Col-I, ALP, Runx-2, BMP2 and BMP7 established for cultured osteoblasts seeded on the several experimental NPs covered titanium discs, after 48 h. Results were expressed as mean and standard deviation and presented in ng mRNA/ng HK. Different letters indicate significant differences after One-way ANOVA and post-hoc multiple comparisons ($p \leq 0.05$). Control: titanium discs, NPs: Titanium discs covered with un-doped NPs, TDg NPs: Titanium discs with Tideglusib doped NPs, LPS: 1 μg of bacterial endotoxin was added to cultured cells.

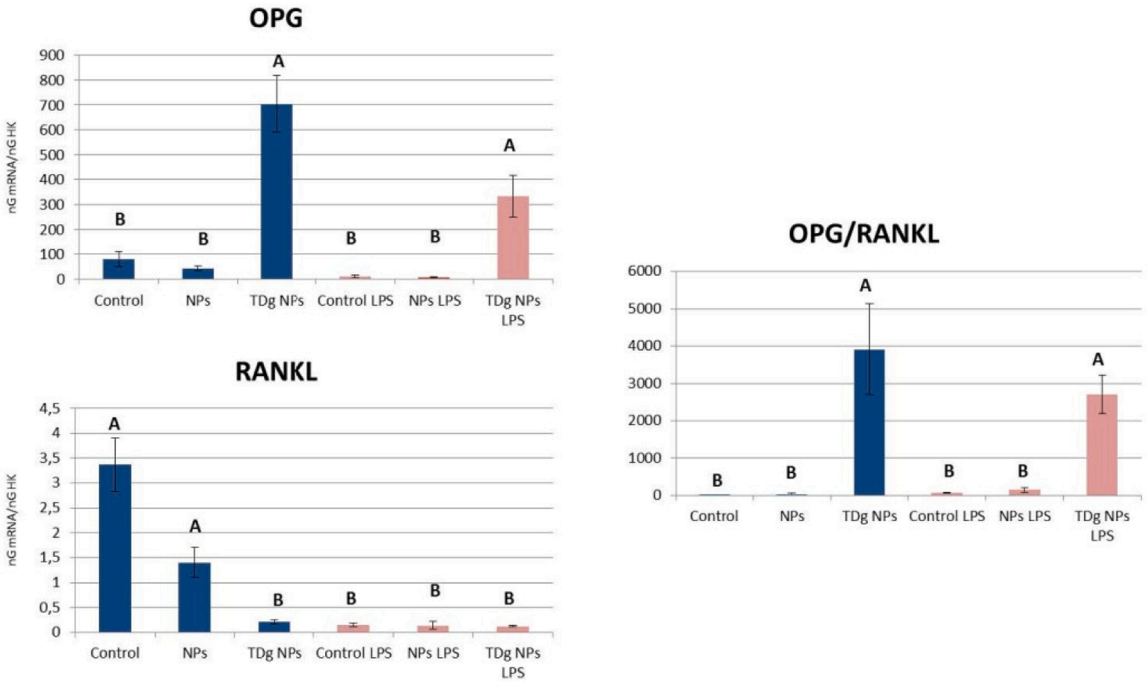

Fig. 5. Quantitative real-time PCR gene expression analysis of RANKL and OPG, established for cultured osteoblasts seeded on the several experimental NPs covered titanium discs, after 48 h. Results were expressed as mean and standard deviation and presented in ng mRNA/ng HK. OPG/RANKL ratio is also displayed. Different letters indicate significant differences after One-way ANOVA and post-hoc multiple comparisons ($p \leq 0.05$). Control: titanium discs, NPs: Titanium discs covered with un-doped NPs, TDg NPs: Titanium discs with Tideglusib doped NPs, LPS: 1 μg of bacterial endotoxin was added to cultured cells.

fully covered by osteoblasts with evident surface mineralization (Figs. 6F and 7F).

4. Discussion

This study aimed to evaluate whether the functionalization of titanium surfaces with NPs doped with TDg would counteract the effects of LPS on proliferation and differentiation of human osteoblasts. For this purpose, we obtained and cultured primary osteoblasts from humans and studied their proliferation with MTT assays and by measuring the expression of proliferation-related genes using RT-qPCR. Osteoblasts' differentiation was tested quantitatively by measuring their ALP activity and by measuring the expression of differentiation-related genes (e.g., ALP, OSC, BMP-2, BMP-7, Runx-2 or OSX). The gene expression of the OPG/RANKL ratio was also assessed to determine the osteoblast bone remodelling activity [12]. Finally, the cultured osteoblasts onto the titanium surfaces were evaluated by FESEM to indirectly evaluate the impact of NPs on the osteoblast morphology and cell-to-cell interactions [12].

We used primary human osteoblasts, since they have shown higher reliability, when compared to other tumoral cells lines, despite their limited accessibility and requiring larger isolation times [18,19]. Their proliferation was studied by MTT assay (Fig. 1), which was not affected by undoped-NPs, what demonstrates that these polymeric non-resorbable NPs were not detrimental for osteoblast proliferation, as demonstrated in previous in vitro investigations [12,20]. These osteoblasts were firmly attached to the Ti surfaces covered by NPs, and after 48 h, spread onto the disks, as shown by FESEM (Figs. 6B and 7B).

TDg-NPs were not only detrimental for osteoblasts proliferation, but demonstrated a double-fold increase. This effect may be explained by the GSK-3β inhibition, which may activate the Wnt/β-catenin signaling pathway, which directly leads to the proliferation of osteoblasts [7,8]. Furthermore, some of the proliferation-related genes tested by RT-qPCR analysis, as TGF-β1, TGF-βR1, TGF-βR2 and TGF-βR3, were up-regulated by the TDg-NPs (Fig. 4). This effect may be the coordinated activity between Wnt/β-catenin and TGF-β pathways during osteoblast proliferation [21]. With FESEM a high osteoblasts proliferation with production of abundant extracellular matrix was also observed in presence of TDg-NPs (Figs. 6E and 7E).

TDg-NPs induced an overexpression of Runx-2 gene expression. Previous investigations have shown that Osteoblasts with an up-regulated metabolic activity are characterized by high Runx-2 and osterix levels, with an increased alkaline phosphatase activity [22]. This overexpression of Runx-2 is performed under inhibition of the β-catenin degrading enzyme -GSK-3β-, thus increasing the OPG/RANKL ratio, and hence promoting bone formation [22]. GSK3-β also leads to inhibition of Runx-2 by inducing its phosphorylation [23]. Thus, targeting the GSK3-β pathway is an efficient mode to reverse a detrimental effect on osteoblasts differentiation. This effect of TDg trough down-regulation of GSK-3β has been shown to increase bone mineral density and new bone area formation by promoting early osteoblast differentiation [6] and diminishing osteoblast apoptosis, [24].

When in presence with LPS (Fig. 1) the osteoblast proliferation was reduced in half, effect which has been previously reported by other authors using primary human osteoblasts, with the same LPS dosage (1 μg/mL) and a similar experimental design on titanium discs [25], in well plates [5], or even with lower LPS concentrations (100 ng/mL) [26]. It was also evident by FESEM that the number of osteoblasts

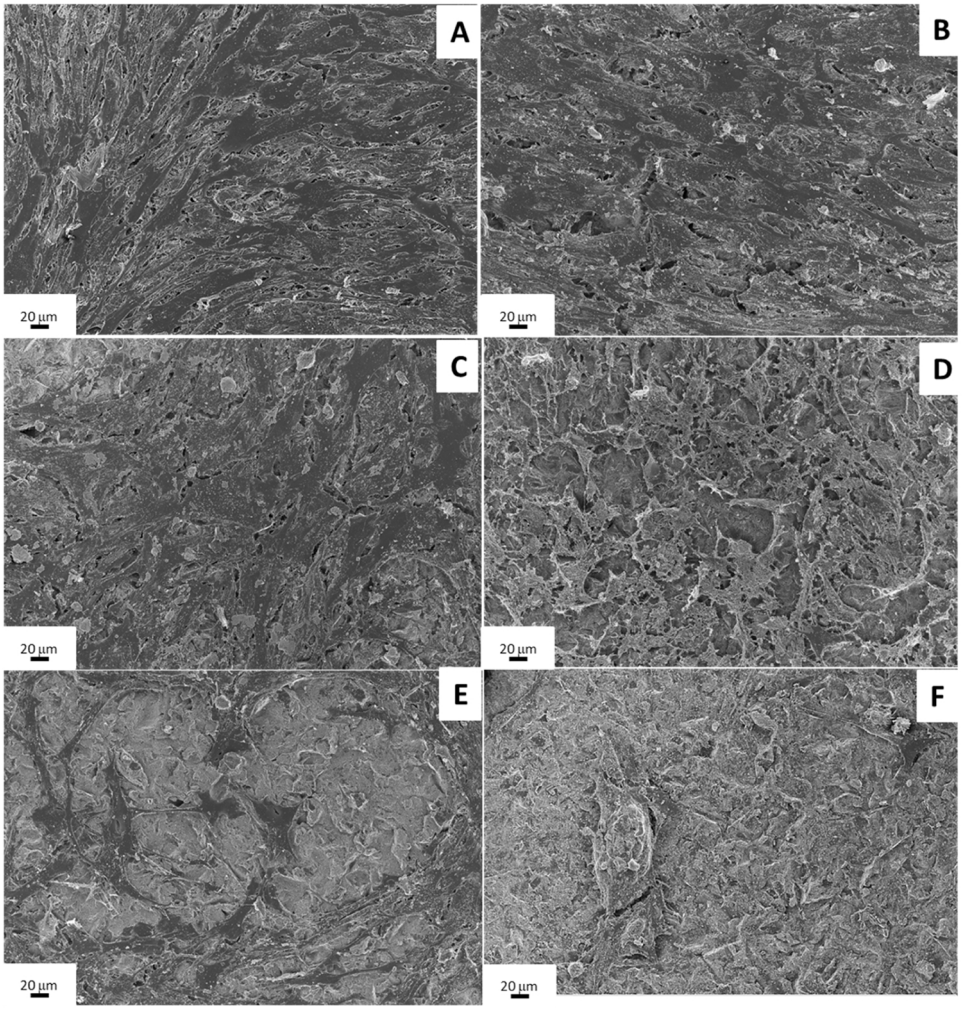

Fig. 6. Low magnification FESEM images of osteoblasts cultured onto Ti discs A) control, B) Ti discs with NPs and C) Ti discs with TDg NPs and pictures of LPS-treated osteoblasts cultured onto D) Ti discs control, E) Ti discs with NPs and F) Ti discs with TDg NPs. Osteoblasts grown without LPS completely cover the titanium surfaces. Osteoblasts grown on TDg NPs are more elongated in shape and extracellular substance production is present. Magnifications were at 500X.

cultured in the presence of LPS diminished and showed signs of membrane cells damage (Figs. 6C and 7C).

In the present study, TDg-loaded NPs were able to counteract this LPS induced effect by increasing three-fold the mean number of the osteoblasts. Other authors have tried without success to counteract this inhibiting effect of LPS on osteoblast proliferation using either enamel matrix derivative (EMD) or hyaluronic acid [5]. LPS promotes cell death by up-regulating GSK-3β, what may explain why the use of TDg (a GSK-3 β inhibitor) was able to counteract the LPS-induced cell death, as previous in vitro experiments have reported through the inactivation of the inflammasome-mediated cell pyroptosis mediated by LPS [3].

Osteoblast differentiation was indirectly evaluated in this investigation by alkaline phosphatase production (Fig. 2). The application of LPS reduced in half ALP production, while in presence with TDg-NPs this drop was partially reversed. The effect of LPS on osteoblast function has been previously reported, by promoting its apoptosis and differentiation inhibiting [27] via activation of the c-Jun N-terminal kinase (JNK) pathway, which functions trough the mitogen-activated protein kinase (MAPK) signaling [28].

LPS did not inhibit the gene expression of Runx-2, ALP, OSX or OPG, while TDg NPs up-regulated these genes. In osteoblast differentiation, two subsequent steps may be distinguished: *i*) the up-regulation of Runx-2 [29], and *ii*) the increase of specific transcriptional factors and osteogenic proteins as ALP, OPG and OSX [30,31]. As previously mentioned, TDg-NPs not only facilitated the over-expression Runx-2, but also the expression of specific osteogenic proteins as ALP, OSX and OPG (Fig. 4), thus demonstrating a similar mechanism as shown with the osteogenic bone morphogenetic proteins (BMPs).

Bone remodeling is regulated by the receptor activator of the NF-kB ligand (RANKL) and osteoprotegerin (OPG) regulate, by either stimulating or inhibiting osteoclasts differentiation, and both have been shown to actively participate in the osseous destruction during peri-implantitis [32]. In the absence of LPS and in presence of TDg-NPs osteoblasts overexpressed OPG and a down-regulated RANKL. The OPG/RANKL ratio in the presence of TDg-NPs demonstrated a 3,000-fold increase compared to the control group. This up-regulation of OPG was also evidenced in the presence of LPS, what may be explained the regulation of the OPG expression in osteoblasts by the Wnt/β-catenin system [33]. TDg-NPs also decreased RANKL gene expression, which is consistent with a previous study reporting down-regulation of the effect of GSK-3, by inhibiting NF-kB activation and hence, limiting the osteoblast response to inflammation expression, which is mediated through β-catenin, [34].

Matrix mineralization was evaluated after 14 and 21 d, and both tested time-points followed the same trend (Fig. 3). As previously described LPS diminished matrix mineralization [25], what is consistent with the described results on the effect of LPS inhibiting osteoblast proliferation, ALP activity and mineralized nodules [35]. However, the inhibition of GSK3-β by TDg-NPs remarkably reduced this inhibition, since even in presence of LPS, it promoted an osteogenic effect

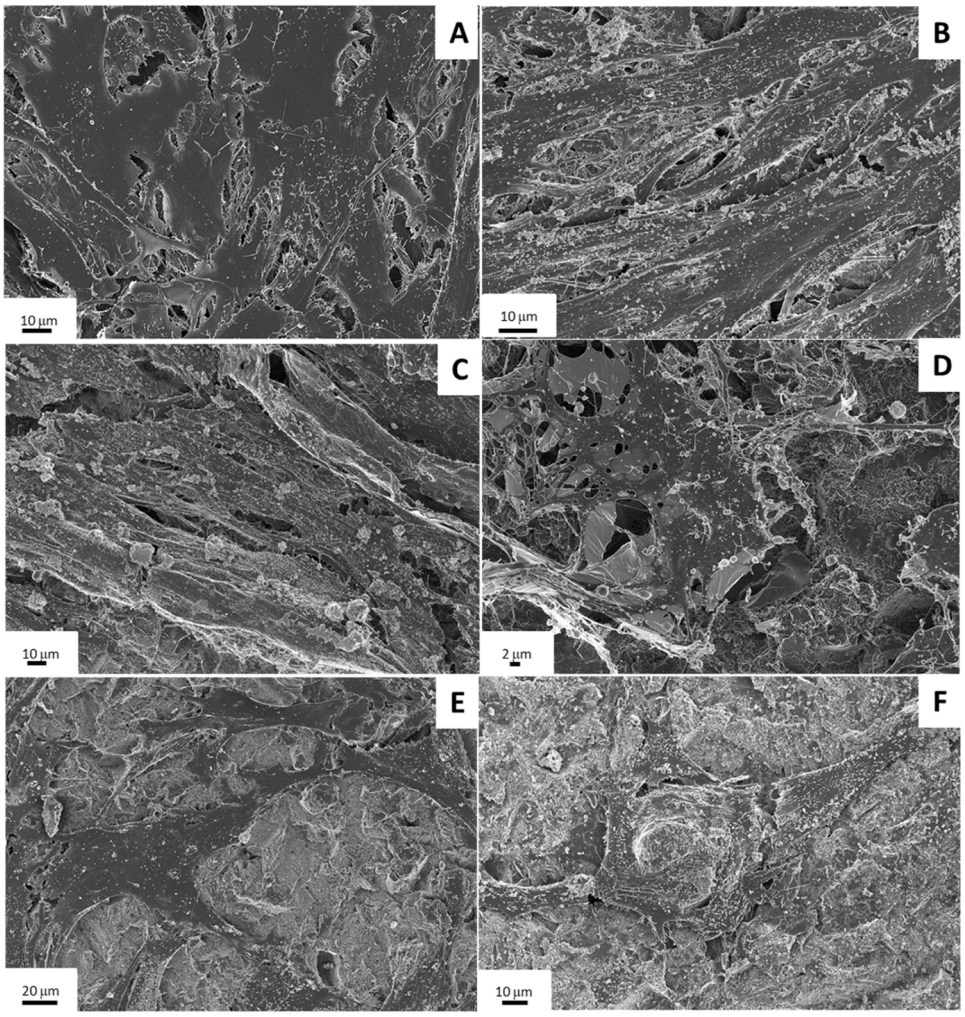

Fig. 7. High magnification FESEM images of osteoblasts cultured onto Ti discs A) control, B) Ti discs with NPs and C) Ti discs with TDg NPs, and pictures of LPS-treated osteoblasts cultured onto D) Ti discs control, E) Ti discs with NPs and F) Ti discs with TDg NPs. Osteoblasts seeded on titanium are flat and polygonal shaped with multiple cytoplasmatic connections. In the presence of LPS, osteoblasts grown on control titanium surfaces have membrane disruption signs. Osteoblasts grown on TDg NPs are elongated in shape and extracellular substance production is clearly noticed. Magnifications were between 1000 and 3,000X.

demonstrated by osteoblast proliferation and differentiation, increased ALP production, as well as increased mineralization as shown in FESEM images (Figs. 6X and 7X), which is in the end a sign of favored [36].

This osteogenic effect of TDg-NPs may be explained by its effect on the three main molecular pathways involved in osteogenesis: i) the BMP-Smads, ii) the Wnt/β-catenin and iii) the mitogen-activated protein kinase (MAPK), since they are usually intertwined and interact with one another promoting osteoblasts proliferation and differentiation [36].

Although this report has the obvious limitations of an in vitro investigation, it has the strength of a thorough evaluation of the effect of TDg-NPs on human osteoblasts, including their proliferation, differentiation, alkaline phosphatase production, and effect on their cell morphology, mineralization and gene expression.

In conclusion the use of the GSK-3 inhibitor TDg in NPs when used to functionalize titanium surfaces was able to attenuate the LPS-inhibitory effects on osteoblasts proliferation while demonstrating osteogenic properties. This effect was exerted by upregulating the Wnt/β-catenin and repressing the NF-kB signaling pathways, although these molecular mechanisms require further investigation. Furthermore, the doping of the NP-12 peptide onto the NPs should be further explored as a potential locally delivered drug in the prevention and treatment of peri-implant diseases.

Declaration of Competing Interest

The authors declare that they have no conflict of interest.

Acknowledgements

Grant PID2020–114694RB-I00 funded by MCIN/AEI 10.13039/501100011033. Authors want to thank Dentsply Sirona for providing the titanium discs (Research Agreement I-OT-21–032).

References

[1] Herrera D, Berglundh T, Schwarz F, Chapple I, Jepsen S, Sculean A, Kebschull M, Papapanou PN, Tonetti MS, Sanz M. EFP workshop participants and methodological consultant. Prevention and treatment of peri-implant diseases-The EFP S3 level clinical practice guideline. J Clin Periodo 2023;50(Suppl 26):4–76. https://doi.org/10.1111/jcpe.13823.

[2] Berglundh T, Armitage G, Araujo MG, Avila-Ortiz G, Blanco J, Camargo PM, Chen S, Cochran D, Derks J, Figuero E, Hämmerle CHF, Heitz-Mayfield LJA, Huynh-Ba G, Iacono V, Koo KT, Lambert F, McCauley L, Quirynen M, Renvert S, Salvi GE, Schwarz F, Tarnow D, Tomasi C, Wang HL, Zitzmann N. Peri-implant diseases and conditions: consensus report of workgroup 4 of the 2017 World Workshop on the Classification of Periodontal and Peri-Implant Diseases and Conditions. J Clin Periodo 2018;45:S286–91. https://doi.org/10.1111/jcpe.12957.

[3] Zhang X, He S, Lu W, Lin L, Xiao H. Glycogen synthase kinase-3β (GSK-3β) deficiency inactivates the NLRP3 inflammasome-mediated cell pyroptosis in LPS-

treated periodontal ligament cells (PDLCs). Vitr Cell Dev Biol Anim 2021;57(4):404–14. https://doi.org/10.1007/s11626-021-00583-5.
[4] Page MJ, Kell DB, Pretorius E. The role of lipopolysaccharide-induced cell signalling in chronic inflammation. Chronic Stress (Thousand Oaks) 2022;6:24705470221076390. https://doi.org/10.1177/24705470221076390.
[5] Ramenzoni LL, Annasohn L, Miron RJ, Attin T, Schmidlin PR. Combination of enamel matrix derivative and hyaluronic acid inhibits lipopolysaccharide-induced inflammatory response on human epithelial and bone cells. Clin Oral Invest 2022;26(2):1773–83. https://doi.org/10.1007/s00784-021-04152-8.
[6] Comeau-Gauthier M, Tarchala M, Luna JLR-G, Harvey E, Merle G. Unleashing β-catenin with a new anti-Alzheimer drug for bone tissue regeneration. Injury 2020;51:2449–59. https://doi.org/10.1016/j.injury.2020.07.035.
[7] Kornsuthisopon C, Tompkins KA, Osathanon T. Tideglusib enhances odontogenic differentiation in human dental pulp stem cells in vitro. Int Endod J 2023;56(3):369–84. https://doi.org/10.1111/iej.13877.
[8] Oncu B, Yilmaz AM, Yilmaz BK, Altunok EC, Kuru L, Agrali OB. Cytotoxicity and collagen expression effects of tideglusib administration on human periodontal cells: an in-vitro study. Clin Exp Health Sci 2020;10(2):153–62. https://doi.org/10.33808/clinexphealthsci.709924.
[9] Adamowicz K, Wang H, Jotwani R, Zeller I, Potempa J, Scott DA. Inhibition of GSK3 abolishes bacterial-induced periodontal bone loss in mice. Mol Med 2012;18(1):1190–6. https://doi.org/10.2119/molmed.2012.00180.
[10] Neves VCM, Babb R, Chandrasekaran D, Sharpe PT. Promotion of natural tooth repair by small molecule GSK3 antagonists. Sci Rep 2017;7:39654. https://doi.org/10.1038/srep39654.
[11] Yuan P, Qiu X, Liu T, Tian R, Bai Y, Liu S, Chen X, Jin Y. Substrate-independent polymer coating with stimuli-responsive dexamethasone release for on-demand fibrosis inhibition. J Mater Chem B 2020;8:7777–84. https://doi.org/10.1039/d0tb01127d.
[12] Toledano-Osorio M, de Luna-Bertos E, Toledano M, Manzano-Moreno FJ, Costela-Ruiz V, Ruiz C, Gil J, Osorio R. Dexamethasone and doxycycline functionalized nanoparticles enhance osteogenic properties of titanium surfaces. Dent Mater 2023;39(6):616–23. https://doi.org/10.1016/j.dental.2023.05.004.
[13] Bueno J, Virto L, Toledano-Osorio M, Figuero E, Toledano M, Medina-Castillo AL, Osorio R, Sanz M, Herrera D. Antibacterial effect of functionalized polymeric nanoparticles on titanium surfaces using an in vitro subgingival biofilm model. Polym (Basel) 2022;14:358. https://doi.org/10.3390/polym14030358.
[14] Medina-Castillo AL. Thermodynamic principles of precipitation polymerization and role of fractal nanostructures in the particle size control. Macromolecules 2020;53:5687–700. https://doi.org/10.1021/acs.macromol.0c00973.
[15] Manzano-Moreno FJ, Rodríguez-Martínez JB, Ramos-Torrecillas J, Vallecillo-Capilla MF, Ruiz C, García-Martínez O, Reyes-Botella C. Proliferation and osteogenic differentiation of osteoblast-like cells obtained from two techniques for harvesting intraoral bone grafts. Clin Oral Invest 2013;17(5):1349–56. https://doi.org/10.1007/s00784-012-0811-4.
[16] Reyes-Botella C, Montes MJ, Vallecillo-Capilla MF, Olivares EG, Ruiz C. Antigenic phenotype of cultured human osteoblast-like cells. Cell Physiol Biochem 2002;12(5-6):359–64. https://doi.org/10.1159/000067906.
[17] Olvera-Huertas AJ, Costela-Ruiz VJ, García-Recio E, Melguizo-Rodríguez L, Illescas-Montes R, Reyes-Botella C, Manzano-Moreno FJ. The effect of chlorhexidine, amoxicillin, and clindamycin on the growth and differentiation of primary human osteoblasts. Int J Oral Maxillofac Implants 2022;37(2):283–8. https://doi.org/10.11607/jomi.9253. PMID: 35476856.
[18] Czekanska EM, Stoddart MJ, Richards RG, Hayes JS. In search of an osteoblast cell model for in vitro research. Eur Cell Mater 2012;24:1–17. https://doi.org/10.22203/ecm.v024a01.
[19] Toledano-Osorio M, Manzano-Moreno FJ, Ruiz C, Toledano M, Osorio R. Testing active membranes for bone regeneration: a review. J Dent 2021;105:103580. https://doi.org/10.1016/j.jdent.2021.103580.
[20] Osorio MT, Toledano R, Huang H, Toledano-Osorio M, Osorio R, Huang CC, García-Godoy F. Effect of doxycycline doped nanoparticles on osteogenic/cementogenic and anti-inflammatory responses of human cells derived from the periodontal ligament. J Dent 2023;137:104668. https://doi.org/10.1016/j.jdent.2023.104668.
[21] Vallée A, Lecarpentier Y, Guillevin R, Vallée JN. Interactions between TGF-β1, canonical WNT/β-catenin pathway and PPAR γ in radiation-induced fibrosis. Oncotarget 2017;8(52):90579–604. https://doi.org/10.18632/oncotarget.21234.
[22] Kovács B, Vajda E, Nagy EE. Regulatory effects and interactions of the Wnt and OPG-RANKL-RANK signaling at the bone-cartilage interface in osteoarthritis. Int J Mol Sci 2019;20(18):4653. https://doi.org/10.3390/ijms20184653.
[23] Gunn SA, Kreps LM, Zhao H, Landon K, Ilacqua JS, Addison CL. Focal adhesion kinase inhibitors prevent osteoblast mineralization in part due to suppression of Akt-mediated stabilization of osterix. J Bone Oncol 2022;34:100432. https://doi.org/10.1016/j.jbo.2022.100432.
[24] Lektemur Alpan A, Çalişir M, Kizildağ A, Özdede M, Özmen Ö. Effects of a glycogen synthase kinase 3 inhibitor tideglusib on bone regeneration with calvarial defects. J Craniofac Surg 2020;31(5):1477–82. https://doi.org/10.1097/SCS.0000000000006326. PMID: 32195836.
[25] Ramenzoni LL, Bösch A, Proksch S, Attin T, Schmidlin PR. Effect of high glucose levels and lipopolysaccharides-induced inflammation on osteoblast mineralization over sandblasted/acid-etched titanium surface. Clin Implant Dent Relat Res 2020;22(2):213–9. https://doi.org/10.1111/cid.12884.
[26] Yu HJ, Wang LJ, Huang K, Guo QF, Lin BY, Liu YY, Yu M, Ma GP. PPAR-γ agonist pioglitazone alleviates inflammatory response induced by lipopolysaccharides in osteoblast cells. J Orthop Res 2022;40(11):2471–9. https://doi.org/10.1002/jor.25279.
[27] Bandow K, Maeda A, Kakimoto K, Kusuyama J, Shamoto M, Ohnishi T, Matsuguchi T. Molecular mechanisms of the inhibitory effect of lipopolysaccharide (LPS) on osteoblast differentiation. Biochem Biophys Res Commun 2010;402(4):755–61. https://doi.org/10.1016/j.bbrc.2010.10.103.
[28] Wang Y, Zhang L, Wang K, Zhou H, Li G, Xu L, Hu Z, Cao X, Shi F, Zhang S. Circulating exosomes from mice with LPS-induced bone loss inhibit osteoblast differentiation. Calcif Tissue Int 2022;111(2):185–95. https://doi.org/10.1007/s00223-022-00977-x.
[29] Xu J, Li Z, Hou Y, Fang W. Potential mechanisms underlying the Runx2 induced osteogenesis of bone marrow mesenchymal stem cells. Am J Transl Res 2015;7:2527–35.
[30] Nakashima K, Zhou X, Kunkel G, Zhang Z, Deng JM, Behringer RR, de Crombrugghe B. The novel zinc finger containing transcription factor osterix is required for osteoblast differentiation and bone formation. Cell 2002;108:17–29. https://doi.org/10.1016/s0092-8674(01)00622-5.
[31] Uchihashi K, Aoki S, Matsunobu A, Toda S. Osteoblast migration into type I collagen gel and differentiation to osteocyte-like cells within a self-produced mineralized matrix: a novel system for analyzing differentiation from osteoblast to osteocyte. Bone 2013;52:102–10. https://doi.org/10.1016/j.bone.2012.09.001.
[32] Bostanci N, Ilgenli T, Emingil G, Afacan B, Han B, Toz H, Atilla G, Hughes FJ, Belibasakis GN. Gingival crevicular fluid levels of RANKL and OPG in periodontal diseases: implications of their relative ratio. J Clin Periodo 2007;34:370–6. https://doi.org/10.1111/j.1600-051X.2007.01061.x.
[33] Boyce BF, Xing L. Biology of RANK, RANKL, and osteoprotegerin. Arthritis Res Ther 2007;9:S1. https://doi.org/10.1186/ar2165.
[34] Die L, Yan P, Jun Jiang Z, Min Hua T, Cai W, Xing L. Glycogen synthase kinase-3 beta inhibitor suppresses Porphyromonas gingivalis lipopolysaccharide-induced CD40 expression by inhibiting nuclear factor-kappa B activation in mouse osteoblasts. Mol Immunol 2012;52(1):38–49. https://doi.org/10.1016/j.molimm.2012.04.005.
[35] Kong Y, Zhang Y, Cai Y, Li D, Yi B, Xu Q. METTL3 mediates osteoblast apoptosis by regulating endoplasmic reticulum stress during LPS-induced inflammation. Cell Signal 2022;95:110335. https://doi.org/10.1016/j.cellsig.2022.110335.
[36] Shen MJ, Wang GG, Wang YZ, Xie J, Ding X. Nell-1 enhances osteogenic differentiation of pre-osteoblasts on titanium surfaces via the MAPK-ERK signaling pathway. Cell Physiol Biochem 2018;50:1522–34. https://doi.org/10.1159/000494651.